JULY 12–16 2020 VIRTUAL JOINT AAPM | COMP MEETING EASTERN TIME [GMT-4]

Algorithm for optimization of the x-ray beam and filter parameters in dual-energy imaging systems

I. ROMADANOV[1], M. SATTARIVAND[1,2,3]

[1]Department of Medical Physics, Nova Scotia Health Authority, Halifax, NS,Canada.

[2]Department of Physics & Atmospheric Science, Dalhousie University, Halifax, NS,Canada.

[3]Department of Radiation Oncology, Dalhousie University, Halifax, NS, Canada.

INTRODUCTION

Dual-energy (DE) x-ray imaging has a long history of practical applications [1,2]. It requires acquiring two x-ray images with different spectra. Such spectra can be generated by changing x-ray tube voltage (kVp) and current (mAs). However, this is not enough to provide optimal conditions for high-quality DE acquisition. The conventional method is to introduce filtration of the x-ray beam through materials of varying thickness L and atomic number Z. Various combinations of filter Z and L, and tube kVp and mAs result in DE images with different subject contrast and noise. In this study we propose an algorithm, which determines the optimal x-ray beam and filtration parameters, leading to the maximized quality of DE images, evaluated through the contrast-to-noise ratio.

AIM

This study aims to find optimal filtration for low- and high-energy beams (Z and L) and optimal x-ray tube parameters (kVp and mAs), which provide the maximum contrast-to-noise ratio (CNR), which was chosen as the figure of merit.

The optimization should include clinically related constraints, such as patient size, patient dose, detector dynamic range, and x-ray tube limits. Three patient sizes were considered: small, medium, and large [3]. For each size, the specific dose constraint was used. The dynamic range of ExacTrac (Brainlab AG, Germany) detector was used [3].

METHOD

- A virtual phantom was used (Fig. 1) with geometry similar to the one used in experiments.

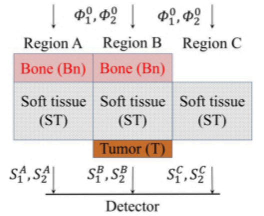

Figure 1. Virtual phantom to calculate CNR. $\Phi_{1,2}^0$ are initial spectra of HE, LE beams with $S_{1,2}^{A,B,C}$ are the resulting signals of the attenuated spectra as incident at the detector for regions A, B, and C respectively.

- Monte Carlo model [4] was used to obtain scatter-to-primary ratios (SPR) for different regions of interest.
- The analytical expression connecting DE CNR with input spectra and SPR was derived.
- Input x-ray spectra for each combination of kVp, mAs, Z, and L were simulated with customized Spektr3.0 software [4].
- Each combination of filter/beam parameters was checked against constraints on the flat panel detector dynamic range, patient sizes, and dose limitations. Constraints were taken from a previous study [3].
- Obtained beam/filter parameters were manually unified, in order to reduce the variations in the choice of filters and their thicknesses, while retaining CNR near the optimal value.
- Partial experimental verification was performed.

ALGORITHM

CNR for the virtual phantom, shown in Fig. 1, is defined as

$$CNR = \frac{\frac{S_1^A}{(S_2^A)^\omega} - \frac{S_1^B}{(S_2^B)^\omega}}{\sqrt{\left(\frac{S_1^A}{(S_2^A)^\omega}\right)^2\left[\left(\frac{\sigma_1^A}{S_1^A}\right)^2 + \omega^2\left(\frac{\sigma_1^A}{S_1^A}\right)^2\right] + \left(\frac{S_1^B}{(S_2^B)^\omega}\right)^2\left[\left(\frac{\sigma_1^B}{S_1^B}\right)^2 + \omega^2\left(\frac{\sigma_1^B}{S_1^B}\right)^2\right]}}.$$

In this equation, signal S_i was related to the input spectrum $\Phi(E)$ as

$$S_i = (1 + SPR)\int_0^{E_i^{max}} \Phi_i(E)e^{-\sum \mu_i^k(E)t_k} E\,dE \sim f(Z, L, mAs),$$

and noise σ_i is

$$\sigma_i^2 = (1 + SPR)\int_0^{E_i^{max}} \Phi_i(E)e^{-\sum \mu_i^k(E)t_k} E^2\,dE \sim f(Z, L, mAs).$$

Calculations were performed for a combination of low and high energy (E_1^{max} and E_2^{max}) beams from 60 to 140 kVp with 10 kVp increments. Current, filter material and thickness were varied independently for low and high energies. Tube current varied from 1 to 90 mAs (ExacTrac limits). Filter thickness L varied from 0 to 2.0 mm with 0.2 mm increments. Filter materials were selected from the periodic table, with Z from 1 to 83, except for radioactive, gases, liquids, and highly reactive elements. For one energy pair these parameters form a 6D space. At each point, three quantities were calculated: CNR, equivalent surface dose (ESD), and air kerma at the detector surface

$$CNR \sim f(Z_1, L_1, mAs_1, Z_2, L_2, mAs_2),$$
$$ESD \sim f(Z_1, L_1, mAs_1, Z_2, L_2, mAs_2),$$
$$Air\ kerma \sim f(Z_1, L_1, mAs_1, Z_2, L_2, mAs_2).$$

ESD was calculated as per AAPM TG-61 protocol, and the dose constraint was such that the DE dose is less than clinically established single energy dose. Detector dynamic range is expressed in terms of air kerma at the detector surface. The resulting data was represented as nested cubes, where each cube is in Z, L, mAs coordinates.

After the constraints were applied (Fig. 2) the maximum CNR value was found, and the corresponding combination of parameters was obtained. The same procedure was repeated for each combination of kVp and the overall maximum was determined. The same procedure was repeated over all patient sizes.

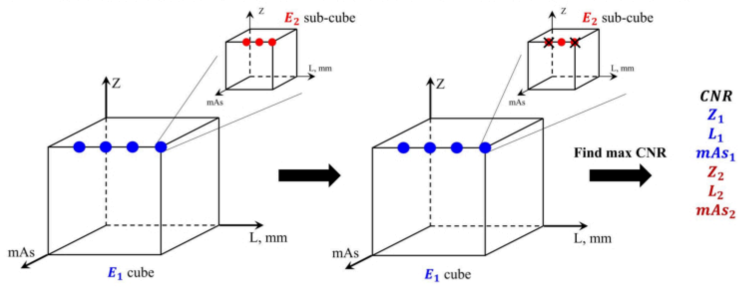

Figure 2. Algorithm flow and data representation. On the left, there is a "cube" in Z_1, L_1, mAs_1 coordinates. Each point is a "sub-cube" in Z_2, L_2, mAs_2. Each point in this "sub-cube" is the CNR, $Dose$ or $Air\ kerma$ value.

ACKNOWLEDGEMENTS

The authors would like to thank Alan Spurway for help with Monte Carlo simulations and Sahar Darvish-Molla for fruitful discussions. This work was supported by:

Atlantic Canada Opportunities Agency | Agence de promotion économique du Canada atlantique

RESULTS

ALGORITHM'S DATA REPRESENTATION

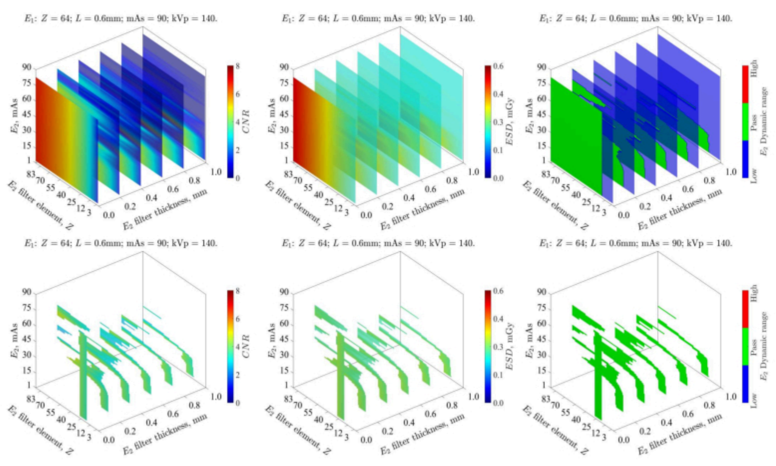

Figure 3. Top row: 3D "cube" of CNR, ESD, and dynamic range ($Air\ kerma$) for one set of Z_1, L_1, mAs_1 parameters. Bottom row CNR, ESD, and dynamic range ($Air\ kerma$) with applied system constrains.

OPTIMAL SPECTRA

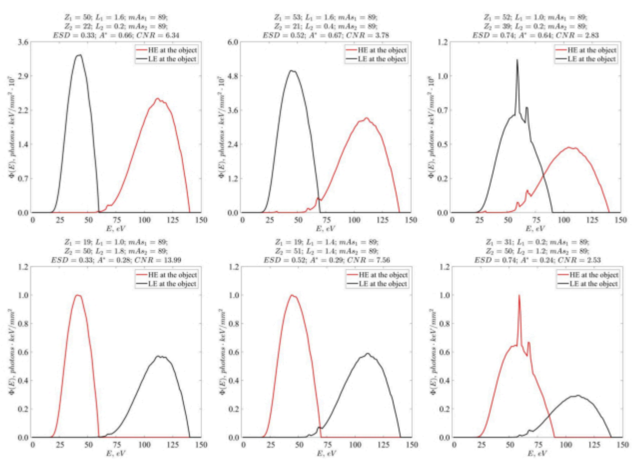

Figure 5. Top row: optimal spectra for soft-tissue only images. Bottom row: optimal spectra for bone only images. From left to right: high, medium, and large patient sizes.

ADJUSTED NEAR OPTIMAL PARAMATERS

Table 1: Near-optimal DE filtration parameters for sot-tissue images

Size	Beam				Filter				A^*	CNR
	kVp		mAs		Z		L			
	E_1	E_2	E_1	E_2	E_1	E_2	E_1	E_2		
Small	140	60	75	80	47	22	1.0	0.2	0.32	6.13
Medium	140	70	90	90	47	22	1.0	0.2	0.68	4.81
Large	140	90	90	90	47	22	1.0	0.2	0.77	2.69

Table 2: Near-optimal DE filtration parameters for bone-only images

Size	Beam				Filter				A^*	CNR
	kVp		mAs		Z		L			
	E_1	E_2	E_1	E_2	E_1	E_2	E_1	E_2		
Small	60	140	80	70	22	47	0.2	1.0	0.4	19.46
Medium	70	140	90	90	22	47	0.2	1.0	0.32	11.80
Large	80	140	90	90	22	47	0.2	1.0	0.23	4.81

Table 3,4: DE parameters for soft tissue (*top*) and bone (*bottom*) only images with no filtration

Size	Beam				A^*	CNR
	kVp		mAs			
	E_1	E_2	E_1	E_2		
Small	140	60	4	62	0.61	2.89
Medium	140	70	7	57	0.57	1.96
Large	140	90	6	51	0.74	1.29

Size	Beam				A^*	CNR
	kVp		mAs			
	E_1	E_2	E_1	E_2		
Small	60	140	62	4	0.39	14.30
Medium	60	140	90	7	0.43	9.17
Large	80	140	63	8	0.34	3.25

PHANTOM AND FILTERS

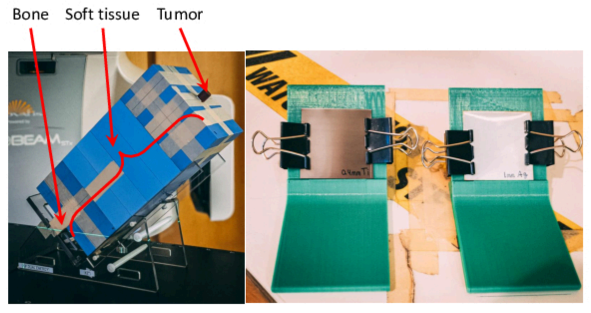

Figure 6. Left: Phantom representing large patient size (40 cm soft tissue, 3 cm of bone). Right: Titanium and silver filters (note that results were obtained with 0.2mm Ti filter). Filters were installed on a 3D printed holder, to compensate for the oblique angle.

EXPERIMENTAL RESULTS

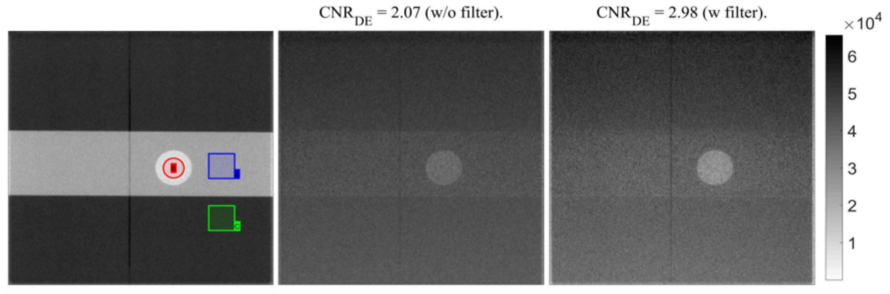

Figure 7. From left to right: Single energy image, DE with no filtration, DE with filtration. ROI A and C used to calculate bone cancellation weighting factor, ROI A and B to calculate CNR. Data for medium size patient.

DISCUSSION AND CONCLUSIONS

The developed algorithm allows for optimization of the filtration and beam parameters, leading to maximized CNR, while considering all clinical constraints, such as patient dose, detector dynamic range, and x-ray tube operational ranges. The core of the algorithm is the expression, which relates input spectra to the output DE image CNR. This model has several simplifications. First, scatter contribution was included by using the scatter-to-primary ratio, without considering the energy shift between primary and scattered photons. Second, the detector is assumed ideal, and the noise was estimated without considering the detector's quantum efficiency, energy absorption, read-out noise, or scatter contributions. Full experimental verification is undergoing (delayed due to COVID-19); nonetheless, the preliminary experimental results showed that materials identified by the algorithm indeed increase the image CNR.

The algorithm is implemented in Matlab and determines the optimal set of parameters by computing over 10^9 possible combinations. In order to optimize execution time, the Matlab parallelization toolbox was used. The average run time for one patient size for one type of image (bone or soft-tissue) was reduced to about 1.5 hours. The total optimization time (all patient sizes, bone, and soft tissue images) is about 9 hours.

Optimization was conducted for ExacTrac system parameters, but the algorithm, in general, can be implemented for any system. The optimal filtration pair was identified for each patient's size. This resulted in a combination of three pairs of filters with different materials and thicknesses. This set was reduced to a combination of two materials with different thicknesses, namely:

^{47}Ag, 1.0mm for HE and ^{22}Ti, 0.2mm for LE.

Corresponding optimal beam parameters can be found in Tables 1,2.

REFERENCES

1. Alvarez RE, Extraction of energy dependent information in radiography PhD thesis Dept. of Electrical Engineering, Stanford University, 1976.
2. Alvarez RE and Macovski A Energy-selective reconstructions in x-ray computerized tomography, Physics in Medicine & Biology 21(5), 733(44), 1976.
3. Darvish-Molla S , Spurway AJ, Sattarivand M, Comprehensive characterization of ExacTrac stereoscopic image guidance system using Monte Carlo and Spektr simulations, Physics in Medicine & Biology, 2020.
4. Punnoose J, Xu J, Sisniega A, Zbijewski W, and Siewerden JH, Technical note: SPEKTR 3.0 a computational tool for x-ray spectrum modeling and analysis Medical Physics 43(8), 471117, 2016

CONTACT INFORMATION

Ivan.Romadanov@nshealth.ca, Mike.Sattarivand@nshealth.ca